JOURNAL OF MATERIALS SCIENCE 29 (1994) 3665–3672

The effect of grain-boundary devitrification on the wear of glass-bonded alumina ceramics

M. A. STOUGH, J. R. HELLMANN, J. C. CONWAY JR
Center for Advanced Materials, The Pennsylvania State University, University Park, PA 16802, USA

The steady-state wear behaviour of a 94 wt% alumina was investigated in the as-fired condition and after a post-sintering heat treatment. The post-sintering heat treatment yielded devitrification of the 6 wt% calcia–magnesia–alumino–silicate ($CaO \cdot MgO \cdot Al_2O_3 \cdot SiO_2$) glass grain-boundary phase. In addition, the effect of surface finishing on the wear behaviour of as-fired and heat-treated samples was studied. Steady-state wear rates were determined using a single-pin-on-disc tribometer. The results indicated that heat treated, unfinished samples exhibit a higher steady-state wear rate than as-fired, unfinished samples. The differences observed may arise in response to one or more of the following mechanisms: (i) creation of intergranular thermoelastic stresses due to thermal-expansion mismatch among intergranular species, (ii) elimination of the lubricative glass phase in devitrified specimens, and (iii) elimination of the advantageous effects of viscoplastic deformation of the intergranular glassy phase on stress relaxation. Surface finishing further increased the steady-state wear rate of the heat-treated samples only, and it correlated with an increase in subsurface microcracking and grain pull-out. A lubricative glass film was found to persist on all sample wear tracks, suggesting that the differences in wear behaviour are dominated by intergranular fracture and grain pull-out.

1. Introduction

Traditionally, the material of choice for applications involving wear and friction is a strengthened metal or alloy, generally with the aid of a lubricant. However, advanced ceramic materials also offer unique advantages as tribomaterials. Compared to conventional alloys, ceramics can withstand higher operating temperatures, they provide significant weight reductions and they offer improved corrosion resistance when subjected to wear situations. Because of these and other improved properties, ceramic materials are increasingly being applied in engines, space structures, bearings, cryogenic refrigerators and other technological applications [1]. However, the lack of reliable and accurate databases, as well as the lack of a thorough understanding of the microstructural and compositional characteristics which govern the wear behaviour of ceramics has limited their use as tribomaterials. This study focuses on understanding the role of the grain-boundary characteristics and the surface finish in the wear of glass-bonded aluminium oxide.

Alumina (Al_2O_3) is a prime triboceramic candidate due to its wide availability and relative ease of fabrication. Dong *et al.* [2] investigated the wear behaviour of high-purity alumina ($> 99\%$) as a function of contact load and temperature, and represented the results in the form of wear-transition diagram (Fig. 1) which distinguishes four regions based on their wear characteristics and mechanisms. Regions I, II and III were found to be mild-wear regions ($k < 10^{-6}$); only region IV showed severe wear ($k > 10^{-4}$), where k is the dimensionless wear coefficient or factor defined as [3]

$$k = \frac{WH_0}{FD} \quad (1)$$

where W is the wear volume at sliding distance (m^3), H_0 is the hardness at room temperature ($N\,m^{-2}$), F is the normal load (N), and D is the sliding distance (m).

The wear mechanisms in these regimes include: local plastic deformation and plowing (region I), tribochemical reactions with water (region II) and development of a silicon-rich layer (region III). The severe-wear region (IV) is characterized by intergranular, and some transgranular, fracture. Since it is apparent that fracture and deformation play an important role in governing the wear behaviour of alumina, particularly in regions I and IV, treatments which modify the ceramic's resistance to fracture or its ability to redistribute stress during wear may be expected to modify the wear behaviour as well. Furthermore, modifications which alter the ability of the ceramic to form *self-lubricative* films, such as those observed in Region III, may significantly modify the wear characteristics.

Because most ceramics, including alumina, are produced in polycrystalline form, the need to more closely examine the role of the grain boundaries on the wear characteristics is apparent. Many commercially available aluminas are intentionally formulated with as

0022–2461

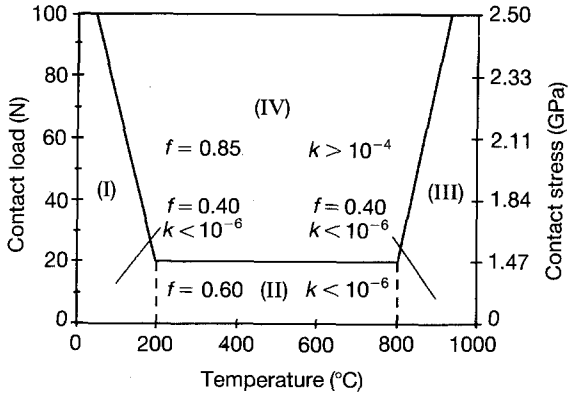

Figure 1 A wear-transition diagram indicating regions of mild wear (regions I–III) and severe wear (region IV) for alumina (Al_2O_3). f is the coefficient of friction and k is the wear coefficient; a large k-value signifies more extreme wear conditions. (After Dong *et al.* [2].)

much as 15 wt % of the binder phase, typically composed of a $CaO \cdot MgO \cdot Al_2O_3 \cdot SiO_2$ glassy material in the grain boundaries. This glassy phase is present to promote liquid-phase sintering, thereby enabling densification of the ceramic to occur at significantly lower temperatures during component manufacturing. In addition, the glass grain-boundary phase permits joining of the ceramic to other components in a subassembly, using conventional metallization and brazing technology [4–6]. Therefore, the glass grain-boundary phase performs an important technological role in the application of this material as a tribo-material.

However, the presence of glass in the grain-boundary has been shown to govern the microstructural development and mechanical properties of aluminas [7–11]. Furthermore, exposure of these materials to elevated, in-service temperatures can yield significant modification in the characteristics of the grain-boundary phase; most notably, devitrification (crystallization) of the glass at temperatures in the range of 900 to 1400 °C has been observed [9–13]. For example, Hellmann *et al.* [10, 11] demonstrated that as-fired 94 wt % alumina exhibited a higher inert strength, but a lower fracture toughness, in the large-flaw regime relative to a devitrified sample of the same material. In addition, devitrification of the grain-boundary significantly improved the alumina's resistance to environmentally enhanced slow crack growth. Because these mechanical properties, which govern the failure behaviour of these aluminas, can be altered markedly by grain-boundary devitrification, it is expected that devitrification will also affect the wear behaviour.

As mentioned earlier, prior studies of wear in alumina have revealed that intergranular fracture and grain pull-out are important contributors to the wear process in aluminas. However, the formation of a lubricative, silica-rich glass film on the wear surface has also been observed in recent studies; this is presumably attributable to the migration of glass from the grain boundaries to the wear surface during the significant localized frictional heating that accompanies the wear process [1, 3, 14]. The observation of transient frictional heating during wear in alumina is not unprecedented [15–16]; however, its role in localized relief of thermoelastic and applied mechanical stresses via viscoplastic deformation of glassy grain-boundaries during wear of alumina has not been fully addressed. Modification of grain-boundary characteristics, such as devitrification, can therefore also modify the wear behaviour by either the elimination of the lubricative glass film or by altering the ability of the grain boundary to relieve applied stresses via viscoplastic deformation during the wear process.

Therefore, we postulate that differences in wear behaviour due to devitrification of the glass grain-boundary phase in alumina may be attributed to some combination of the following: (i) changes in the mechanical properties (strength, fracture toughness, and/or fatigue resistance) of the material; (ii) elimination of the lubricative glass film on the wear surface; or (iii) the decreased capability of the devitrified grain boundary to relieve applied stresses via viscoplastic deformation. In this study, we subjected a 94 wt % alumina to a post-sintering heat treatment designed to devitrify the glass grain-boundary phase. Steady-state wear rates, w, determined using a single pin-on-disc tribometer, were compared for samples before and after the devitrification heat treatment. Qualitative arguments are presented as to the role of grain-boundary devitrification on the wear of the material.

2. Experimental procedure

A commercially available alumina (Coors AD94 alumina, Coors Ceramics Company, Golden, CO 80401, USA) was chosen for this study. This alumina contained 94 wt % aluminium oxide with the balance consisting of 6 wt % calcia–magnesia–alumino–silicate glassy material distributed in the grain boundaries. The alumina was supplied in disc form with diameters of 25.4 mm and nominal thickness of 2 mm. The discs were fabricated from powders via dry isostatic pressing at 165.5 MPa followed by sintering at 1653 °C for 3 h in air. The average density was determined to be 3.70 ± 0.03 g c.c. via Archimedes principle. To complete the wear couple, alumina (Coors AD998 alumina, Coors Ceramics Company, Golden, CO 80401, USA) pins were machined from sintered rods to dimensions of: 3.25 mm in diameter and 14 mm in length. The tip of each pin was machined to a frustum or truncated-cone design with a 45° taper, as schematically illustrated in Fig. 2. The average pin density was 3.95 ± 0.01 g c.c.

The as-fired microstructure of the Coors AD94 alumina, after polishing to a < 0.5 μm diamond finish and thermally etching the sample at 1400 °C for 1 h in air, is shown in Fig. 3. The intergranular glass phase appears dark, while the alumina grains are white with an acicular morphology. The typical grain size and aspect ratio, determined by quantitative optical microscopy were 6.36 ± 4.07 μm and 1.75 ± 0.5 μm, respectively (the largest grain size measured was 43 μm). The intergranular glass composition of AD94 alumina was determined using microprobe elemental analysis [17] and the composition appears in Table I.

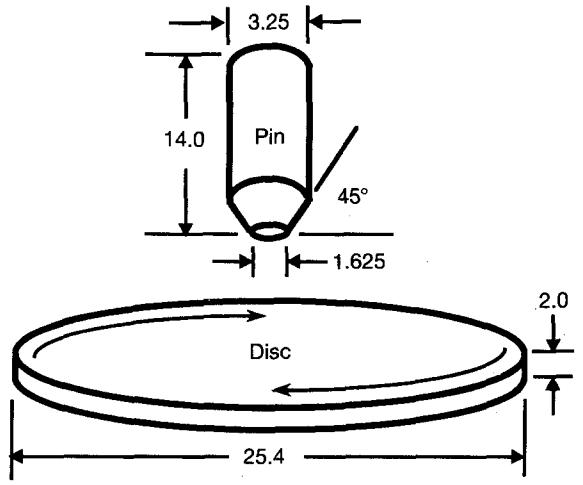

Figure 2 The truncated-cone pin-on-disc arrangement used in this study. All the lengths are in millimetres.

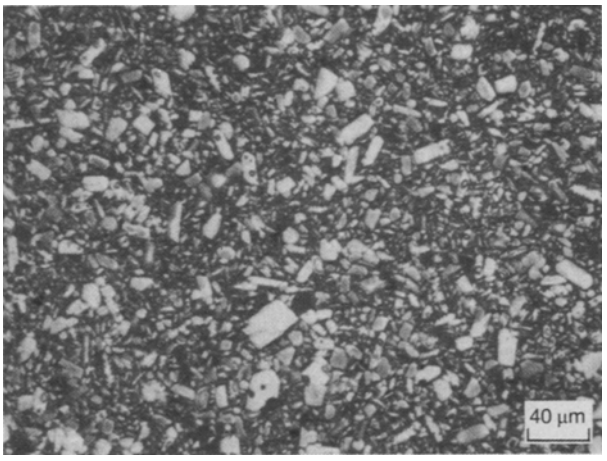

Figure 3 Microstructure of the Coors AD94 alumina after sintering at 1653 °C for 3 h in air, it was thermally etched at 1400 °C for 1 h.

TABLE I Glassy grain-boundary composition of Coors AD94 [17] (determined by electron microprobe analysis, courtesy of Dr Paul F. Hlava, Sandia National Laboratories)

Oxide	Composition mol (%)
SiO_2	44.94 ± 3.49
Al_2O_3	30.59 ± 6.27
MgO	6.58 ± 0.75
CaO	3.42 ± 0.38
Na_2O	1.83 ± 0.10
ZrO_2	1.54 ± 0.26
BaO	8.77 ± 0.92
FeO	0.55 ± 0.05
B_2O_3	0.96 ± 1.01
P_2O_3	0.30 ± 0.12
K_2O	0.26 ± 0.02
TiO_2	0.23 ± 0.02
Cr_2O_3, NiO	Trace
MnO	Not detected

Several as-fired samples were subjected to a post-sintering heat treatment to devitrify the glassy grain-boundary phase. The samples were heated to 1100 °C at 10 °C min^{-1} in a box furnace (Eurotherm Box Furnace, model 4235-3C), then they were held isothermally at 1100 °C for 42.5 h before being cooled at 5° C min^{-1}. The devitrified products were assumed to be similar to those observed previously in an alumina of comparable glass composition [18], and they are presented in Table II. Note the corresponding thermal-expansion coefficients are listed, where available, to rationalize the source of thermoelastic strains that develop in the grain boundary due to differential thermal contraction between various crystalline phases upon cooling from the devitrification treatment.

Several as-fired (AF) and heat-treated (HT) discs were further subjected to a surface-finishing procedure which involved hand lapping one side of each disc. A 45 μm metal-bonded diamond wheel was used as the grinding media and the lapping was performed with water as the lubricant. The samples were rinsed clean in water and acetone and allowed to air dry overnight prior to wear testing.

All wear tests were conducted using a single-pin-on-disc (SPoD) tribometer (schematically illustrated in Fig. 4). In general, the SPoD apparatus mimics the

TABLE II Grain-boundary devitrification products [18] and their respective linear thermal-expansion coefficients [19] (the linear-thermal-expansion coefficient of alumina is 8.8×10^{-6} (°C)$^{-1}$ from 0–1000 °C [20]

Mineral name	Formula	Linear thermal-expansion coefficient ($\times 10^{-6}$ °C^{-1}) (100–200 °C)
Plagioclase (Albite/Anorthite)	$NaAlSi_3O_8/CaAl_2Si_2O_8$	6.3/4.5
Enstatite	$4MgO \cdot 4SiO_2$	13.0
Sapphirine	$2MgO \cdot 2\,Al_2O_3 \cdot SiO_2$	–
Cordierite	$2MgO \cdot 2Al_2O_3 \cdot 5SiO_2$	0.6–2
Residual glass	10–20% of the original composition	–

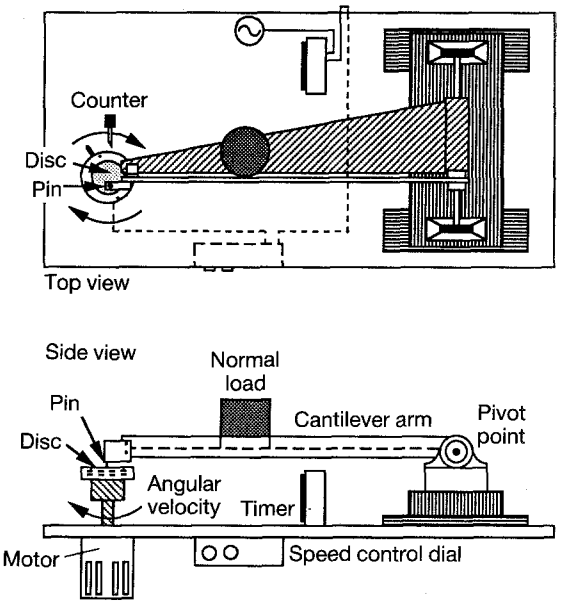

Figure 4 Schematic illustrations of the SPoD tribometer used in this study.

operation of a phonograph turntable. The pin (Fig. 2) was secured in a brass mount which was attached to a tapered aluminium cantilever arm. The position of the pin was such that bending in the cantilever arm was avoided, and since the sample holder was constrained to rotate clockwise (viewed from above), only a tensile force or stress existed in the arm. The disc was clamped in the sample holder, which in turn was attached to a high-torque motor. To establish the conditions for a given wear test, a load was placed on the cantilever arm at a predetermined location in order to achieve a desired contact load of 31.1 N. The sliding velocity was varied using a direct-current (d.c.) motor control dial. After determining the distance of one revolution and the subsequent sliding velocity of 0.074 $m\,s^{-1}$, the total sliding distance was controlled by pre-setting a timer.

Each test began by washing the pin and disc with acetone and drying in air. Each sample was weighed and then inserted into the SPoD. After the cantilever arm, with the pin inserted, was lowered, the wear test commenced. At designated intervals (typically after 100 m of sliding) the disc was removed and washed with acetone, weighed, and then returned to the testing apparatus. All tests were conducted over a total sliding distance of 1000 m, employing the constant-condition test methodology [3]. The cumulative weight loss was plotted as a function of sliding distance in order to determine the steady-state wear rates for each sample type. Fig. 5 illustrates the regions of interest in a typical wear plot generated in this study. Previous studies [22–23] have shown that the wear-in period (region I) varies greatly due to surface topography as well as to differences in the contact load, sliding velocity and temperature. Similarly, we believe that the accelerated-wear period (region III) exhibits non-linearity, and that it can be characterized by the formation of excessive wear debris. Therefore, in order to permit a more reliable and quantitative comparison of the wear behaviour in this study, only the steady-state wear rate, or the slope of the curve in the steady-state wear regime (region II), was addressed. Each curve represents the average of two wear tests under identical conditions. Four sample conditions were evaluated: finished (F) and unfinished (U), as-fired (AF) and heat-treated (HT).

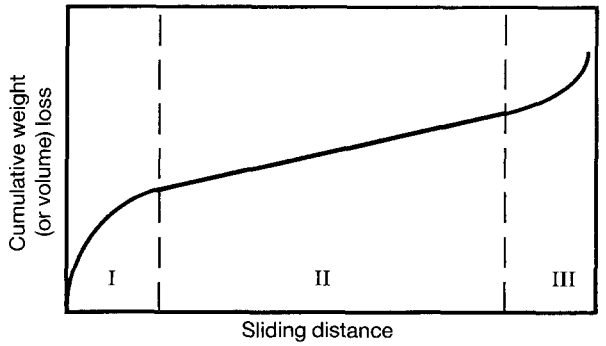

Figure 5 A representation of the wear behaviour for alumina based on data collected in this study and in a previous work [21]. Three regions can be distinguished: I, the wear-in period; II, the steady-state period; and III, the accelerated-wear period.

3. Results and discussion

The initial efforts focused on establishing that the steady-state wear rates obtained in this study agreed well with previously reported values [14, 22–23]. Fig. 6 presents the SPoD data in the form of the cumulative weight loss as a function of the sliding distance for an as-fired, unfinished (AF-U) specimen. Least-squares linear regression was used to fit a line to the steady-state wear region with a slope, hence w, equal to $0.22 \pm 0.11\ \mu g\,m^{-1}$, in acceptable agreement with previously published work by Wang *et al.* [14] and Hsu *et al.* [23] in which a value of $0.37\ \mu g\,m^{-1}$ was reported. The wear coefficient, k, for the as-fired, unfinished specimen was 5.0×10^{-5} (all k-values were determined using 11.5 GPa as the room-temperature hardness of Coors AD94 alumina).

The effect of a devitrification heat treatment on the wear of unfinished discs is shown in Fig. 7. It can be seen from Fig. 7 that the heat treated, unfinished (HT-U) disc exhibits a steady-state wear rate that is more than two times greater than an as-fired, unfinished specimen (AF-U). In addition, k has doubled relative to the as-fired, unfinished specimen. Scanning electron microscopy (SEM) evaluation of the surface microstructure and the wear track of both samples appear similar. No marked difference in the surface microstructure was apparent between as-fired and heat-treated discs prior to wear testing (Fig. 8); more importantly, however, is the presence of a lubricative glass film in the wear track of both as-fired and heat-treated specimens (Fig. 9). A hydrofluoric-acid etch was used to remove a portion of the wear track of both samples, and this confirmed the presence of glass in the wear track of each sample (Fig. 10). Upon closer examination of the wear track where the glass phase has been removed, a higher incidence of inter-granular and transgranular cracks, oriented perpendicular to the direction of rotation, can be observed in the heat-treated specimen. Collectively, these results suggest that the significantly higher steady-state wear rate in

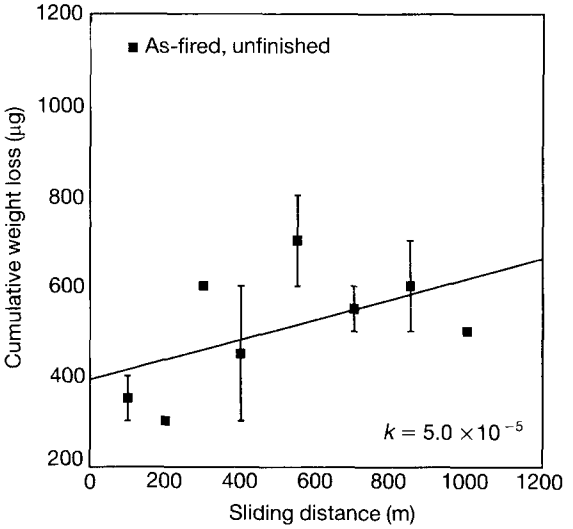

Figure 6 SPoD results for steady-state wear of the ■ as-fired, unfinished alumina specimens (the bars represent the standard deviation from two measurements). $k = 5.0 \times 10^{-5}$, and the linear-regression-fit slope $w = 0.22 \pm 0.11\ \mu g\,m^{-1}$.

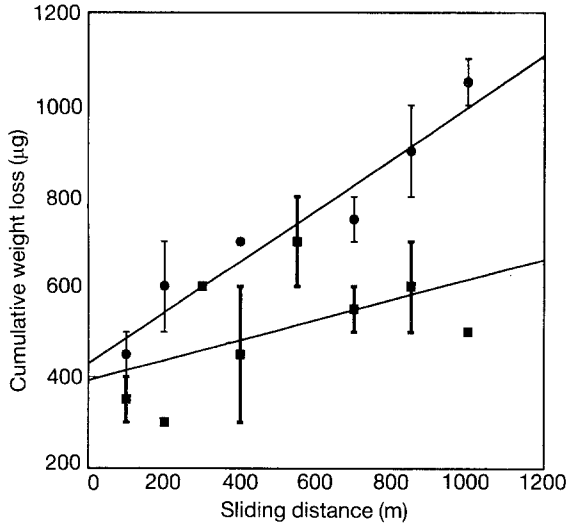

Figure 7 The steady-state wear rates (and wear coefficients) in the unfinished condition of: (●) heat-treated specimens ($w = 0.56 \pm 0.25\ \mu g\ m^{-1}$ and $k = 1.0 \times 10^{-4}$), and (■) as-fired specimens ($w = 0.22 \pm 0.11\ \mu g\ m^{-1}$ and $k = 5.0 \times 10^{-5}$).

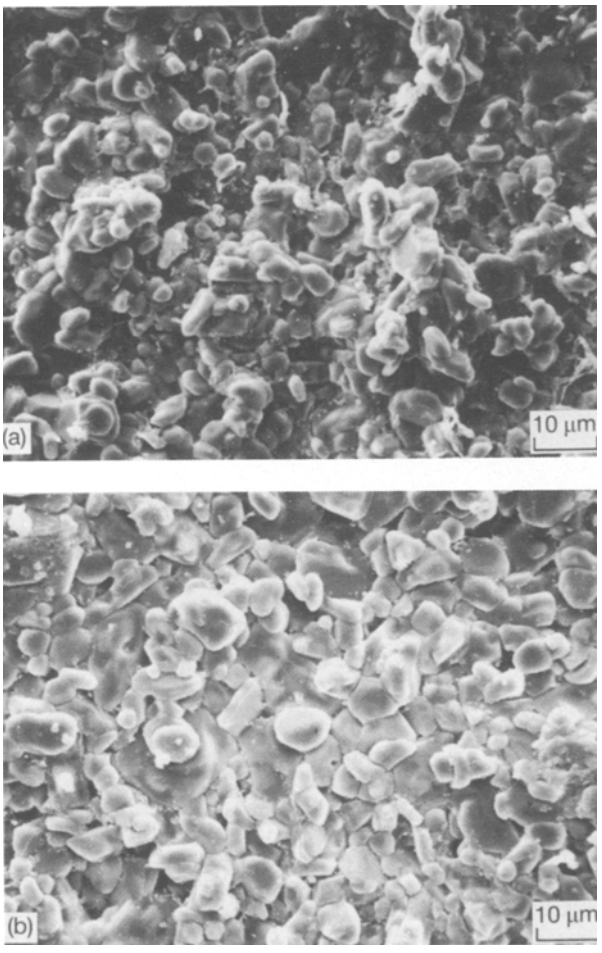

Figure 8 Typical surface morphology observed for (a) as-fired and (b) heat-treated specimens in the unfinished condition prior to wear testing.

the heat-treated specimens cannot be attributed to the absence of a lubricative glass film, but rather it may be due to changes in either the surface topography, the mechanical properties or possibly the residual stress state in the devitrified specimens.

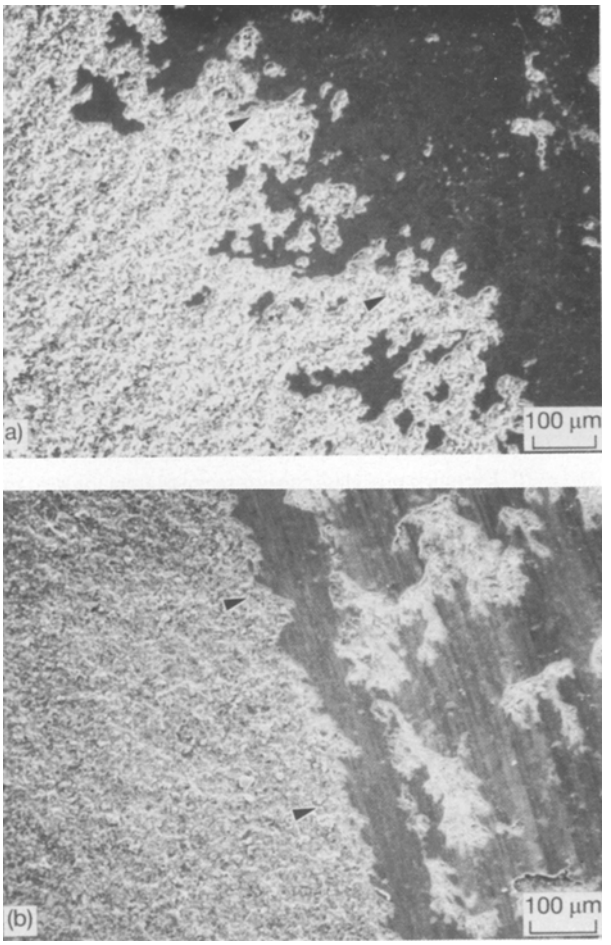

Figure 9 Glass-phase migration to the wear track was observed in both (a) the as-fired and (b) the heat-treated specimens in the unfinished condition. The arrows point to the location of the wear track.

To assess the effect of differences in surface finish on the wear rate, specimens were compared before and after grinding on 45 μm diamond lap. Fig. 11 illustrates that although the magnitude of the wear-in period for the as-fired, finished (AF-F) specimens is significantly lower than for the as-fired, unfinished (AF-U) specimens, the steady-state wear rate for the as-fired specimens remains the same regardless of the degree of surface finish. In contrast, surface finishing yields a three fold increase in the steady-state wear rate for the heat-treated samples, in which the grain boundaries have been devitrified (Fig. 11b). In general, $k_{HT} > k_{AF}$ and comparison with Fig. 1 suggests that heat-treated specimens experience more severe wear conditions than as-fired specimens, which undergo plowing and local plastic deformation at room temperature.

In all finished specimens, the lubricative glass film persists in the wear track (Fig. 12). Previous studies suggest that grain-boundary devitrification is often not complete, and several weight per cent of residual glass can remain after devitrification heat treatments [10–11, 18]. However, a higher incidence of grain pull-out was observed in the heat-treated specimens after surface finishing, relative to as-fired samples (Fig. 13). These results suggest that grain-boundary devitrification yields an increased incidence of intergranular fracture and subsurface damage during the

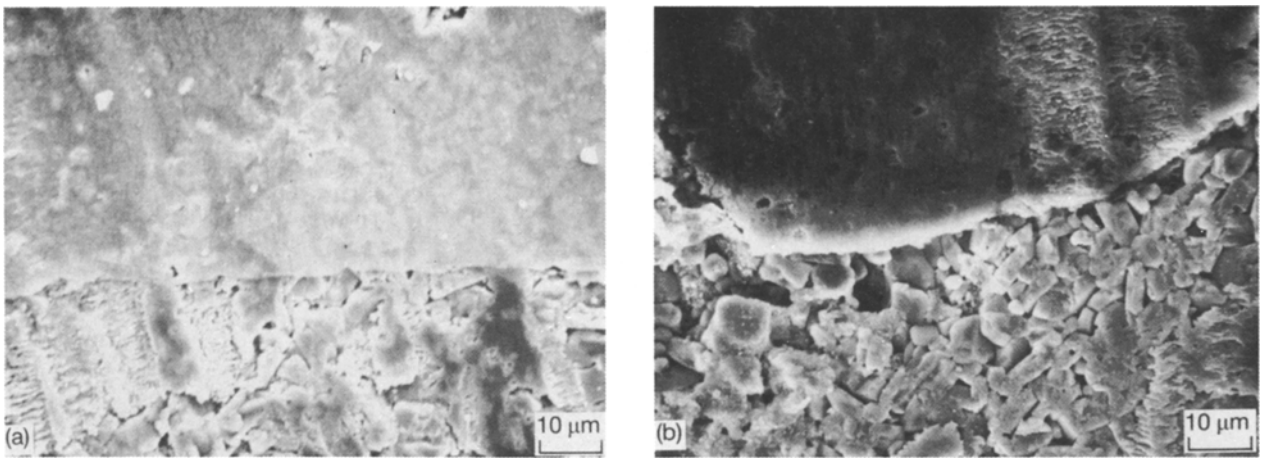

Figure 10 The lubricative glass film was removed from the wear track region via HF etching. A higher incidence of intergranular fracture was observed in the wear track for (a) heat-treated specimens than for (b) as-fired specimens. (The top half of each micrograph is the glass film; the bottom half is the underlying wear-track microstructure).

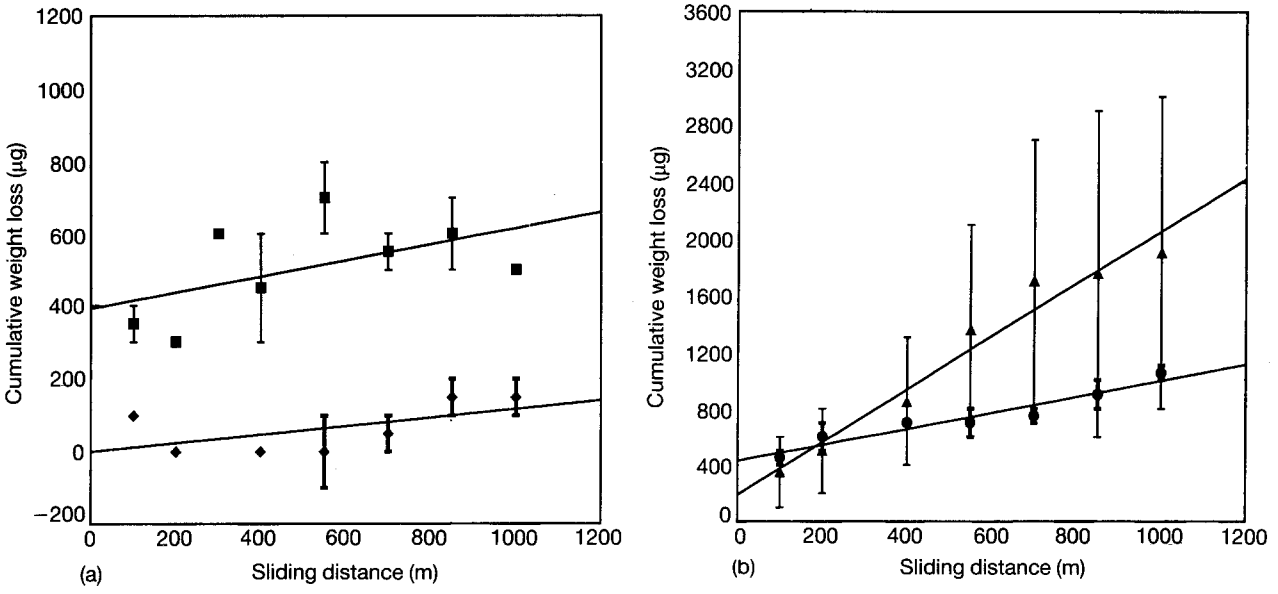

Figure 11 A comparison of the effect of surface finishing on the steady-state wear rate for: (a) as-fired specimens, (◆) finished ($w = 0.12 \pm 0.10\ \mu g\,m^{-1}$ and $k = 1.5 \times 10^{-5}$) and (■) unfinished ($w = 0.22 \pm 0.11\ \mu g\,m^{-1}$ and $k = 5.0 \times 10^{-5}$); and (b) heat-treated specimens, (▲) finished ($w = 1.86 \pm 1.62\ \mu g\,m^{-1}$ and $k = 1.9 \times 10^{-4}$) and (●) unfinished ($w = 0.56 \pm 0.25\ \mu g\,m^{-1}$ and $k = 1.0 \times 10^{-4}$).

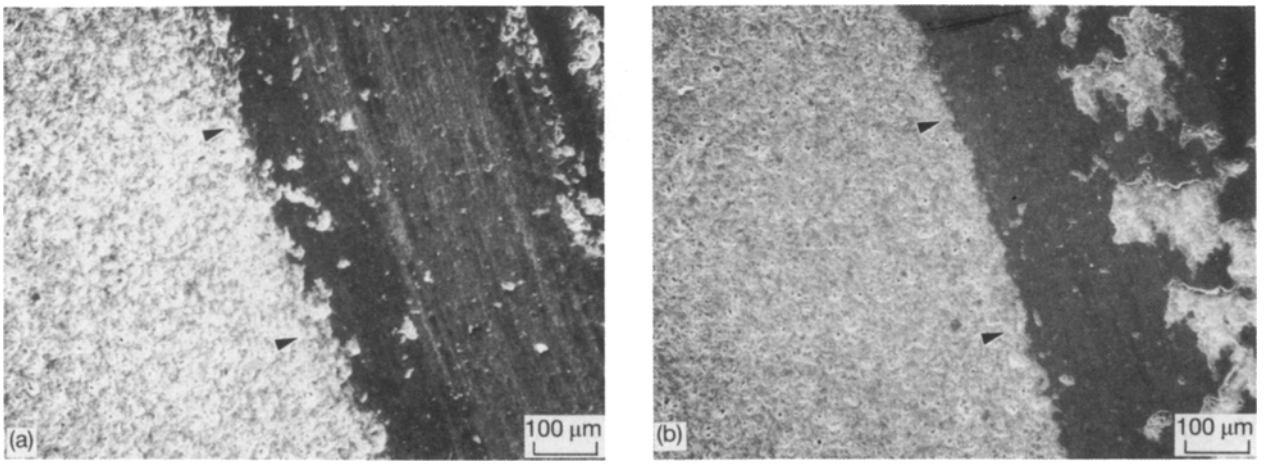

Figure 12 The glass phase persists in the wear track of (a) the as-fired and (b) the heat-treated specimens in the finished condition. The arrows point to the location of the wear track.

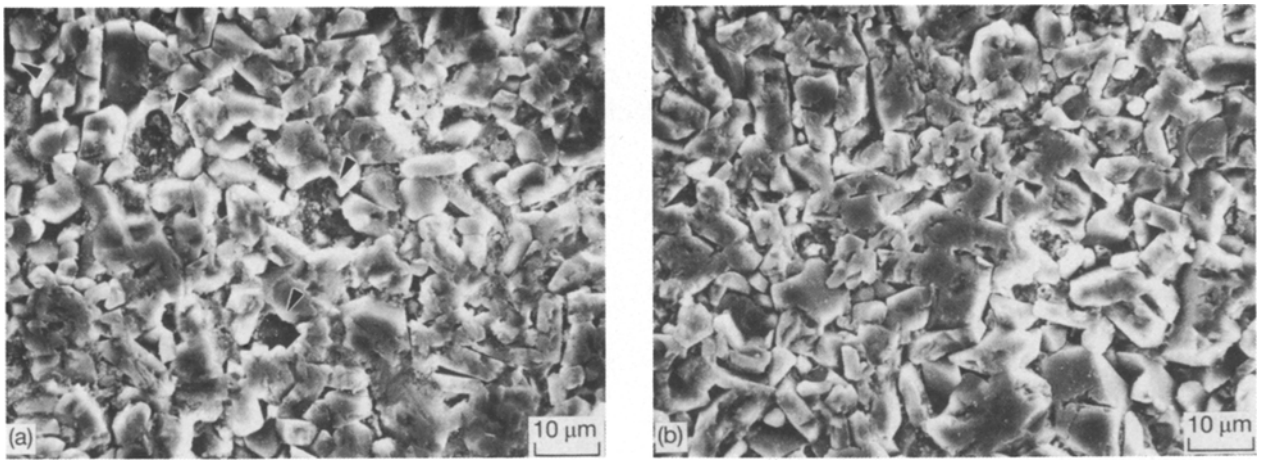

Figure 13 Intergranular fracture and grain pull-out (arrows) is observed below the glass film in the wear track of (a) heat-treated, finished specimens relative to (b) as-fired, finished specimens.

finishing operation, which in turn is manifested as an increased generation of wear debris and a higher steady-state wear rate during testing.

The increased incidence of intergranular fracture and subsurface damage in heat-treated specimens may be attributed to a combination of: (i) a change in the grain-boundary fracture toughness upon devitrification, (ii) establishment of intergranular residual stresses due to differential thermal contraction between devitrified products upon cooling from heat-treatment temperatures, and (iii) modification in the ability of the intergranular phase(s) to relax thermoelastic and applied stresses via viscoplastic deformation.

Recent studies [11–13, 24] have illustrated that the fracture toughness of glass-bonded aluminas can be modified via grain-boundary devitrification. However, the results have indicated that, in general, the macroscopic fracture toughness increases after devitrification particularly in the large-flaw-size regime (significantly larger than the grain size in the aluminas used in this study). Therefore, we believe the greater incidence of pull-out in devitrified samples cannot be attributed to changes in grain-boundary toughness, but rather it may be due to the differences in the intergranular stress state relative to as-fired samples.

Previous studies have also demonstrated that the establishment, and relaxation, of thermoelastic stresses in glass-bonded aluminas are markedly affected by grain-boundary devitrification. Powell-Dogan and Heuer [25, 26], when studying grain-boundary glass crystallization behaviour in 96% alumina, demonstrated that if a MgO/CaO ratio of less than 2 exists in the boundary phase (which is the case for the aluminas in this study, Table I), significant devitrification is expected following an elevated-temperature heat treatment. Powell-Dogan *et al.* [27] later showed that neither residual stresses generated from thermal-expansion mismatch of grain-boundary devitrification products, nor stresses imposed by surface grinding, could, alone, cause the microcracking and grain pull-out observed in their vitreous-bonded aluminas. However, it was suggested that a combination of these stresses may explain the microcracking and grain pull-out observed here. In a separate study, Wong-Ng *et al.* [28] demonstrated a significant increase in residual strain in glass-bonded aluminas upon devitrification of the grain-boundary phase. Such increases in strain (and hence stress) have been correlated with moderate (10–20%) reductions in strength of the material in the small-flaw-size regime [10–11], and, in conjunction with the work of Powell-Dogan *et al.* [27], they may be a potential source of the increased incidence of intergranular fracture and grain pull-out observed in the wear tracks of devitrified specimens examined in this study. However, additional studies of the fracture behaviour of the alumina examined here are required to unambiguously verify this hypothesis.

Finally, recent studies have demonstrated that grain-boundary devitrification markedly alters the ability of glass-bonded aluminas to relax, or redistribute stresses via viscoplastic deformation of the grain-boundary phase [29]. Since thermoelastic stresses induced by grain-boundary devitrification can be superimposed on mechanically applied stresses during surface finishing, the inability of the grain-boundary phase to viscoplastically relax those stresses during the wear test may qualitatively explain the difference in wear behaviour between as-fired and heat-treated specimens.

4. Conclusion

This study has clearly demonstrated that post-sintering heat treatments, intended to devitrify the grain-boundary phase, significantly increase the steady-state wear rate of a glass-bonded alumina ceramic. Surface-finishing procedures, which slightly reduced the wear rates for the alumina in the as-fired condition via removal of surface asperities, yielded a dramatic increase in steady-state wear rates for the heat-treated specimens. Lubricative glass films persisted in the wear tracks of all specimens, indicating that the increased wear rates in heat-treated specimens must be attributed to some other mechanism. An increased incidence of intergranular fracture and grain pull-out was observed in the heat-treated specimens, and con-

tributed to accelerated steady-state wear rates due to debris generation in the wear track. The higher incidence of intergranular fracture is likely to be due to the establishment of thermoelastic stress in the grain boundary due to thermal-expansion mismatch between the devitrification products, alumina grains and residual grain-boundary glass. However, the role of grain-boundary devitrification in reducing the ability of the grain boundary to viscoplastically relax thermoelastic, as well as mechanically applied, stresses during surface finishing and/or wear testing must also be considered in rationalizing the wear-test results.

As a preliminary study focusing on the wear behaviour of glass-bonded alumina after grain-boundary devitrification, the hypotheses discussed above are intended to stimulate further thought in this area. Studies addressing each of the mechanisms proposed to control steady-state wear in these aluminas are necessary to determine which mechanism predominates under a given set of wear conditions, at which point the applicability of alumina as a tribomaterial can be more fully realized.

Acknowledgements

The authors would like to thank Mr John Matsko and Ms Christine Roth, of Sandia National Laboratories for fabricating the alumina specimens.

References

1. D. C. CRANMER, *Tribol. Trans.* **31** (1987) 164.
2. X. DONG, R. S. JAHANMI and S. M. HSU, *J. Amer. Ceram. Soc.* **74** (1991) 1036.
3. Y. S. WANG, S. M. HSU and R. G. MUNRO, *Lubr. Engng* **47** (1991) 49.
4. S. S. COLE Jr and H. W. LARISCH, in "Advances in electron tube techniques", edited by D. Slater, (Pergamon Press, New York, 1961).
5. M. E. TWENTYMAN, *J. Mater. Sci.* **10** (1975) 765.
6. S. S. COLE, Jr and F. J. HYNES, *Bull. Amer. Ceram. Soc.* **37** (1958) 135.
7. W. A. KAYSER, M. SPRISSLER, C. A. HANDWERKER and J. E. BLENDELL, *J. Amer. Ceram. Soc.* **70** (1987) 339.
8. O. H. KWON and G. L. MESSING, *ibid.* **67** (1984) C43.
9. L. REED, in Proceedings of the Sixth National Conference on Tube Techniques, edited by D. Slater (Pergamon Press, New York, 1963) p. 15.
10. J. R. HELLMANN, J. MATSKO, S. W. FREIMAN and T. L. BAKER, in Proceedings of the Twenty-First University Conference on Ceramic Science, The Pennsylvania State University, July 1985, edited by R. E. Tressler, G. L. Messing, C. G. Pantano and R. E. Newnham (Plenum Press, New York, 1985) p. 167.
11. J. R. HELLMANN, S. W. FREIMAN, B. J. HOCKEY and T. L. BAKER, *J. Amer. Ceram. Soc.* (submitted).
12. W. A. ZDANIEWSKI and H. P. KIRCHNER, *Adv. Ceram. Materials* **1** (1986) 99.
13. N. A. TRAVITSKY, D. G. BRANDON and E. Y. GUTMANAS, *Mater. Sci. Engng* **71** (1985) 65.
14. Y. S. WANG, S. M. HSU and R. G. MUNRO, *Lubr. Engng* **47** (1991) 63.
15. I. A. CUTTER and R. McPHERSON, *J. Amer. Ceram. Soc.* **56** (1973) 266.
16. R. McPHERSON, *Wear* **23** (1973) 83.
17. P. F. HLAVA, Sandia National Laboratories (1985) unpublished research.
18. B. J. HOCKEY, in Alumina Processing and Properties Characterization Workshop, Sandia National Laboratories, Report number SAND86-1224C, edited by J. R. Hellmann, p. 43.
19. R. H. STUTZMAN, J. R. SALVAGGI and H. P. KIRCHNER, "Summary report on an investigation of the theoretical and practical aspects of the thermal expansion of ceramic materials", Office of Technical Services, US Department of Commerce PB Washington DC 161826 (1959).
20. W. D. KINGERY, H. K. BOWEN and D. R. UHLMANN, "Introduction to ceramics" (Wiley, New York, 1976).
21. M. WOYDT and K. H. HABIG, *Trib. Int.* **22** (1989) 78.
22. J. L. SPODNIK and J. J. WERT, *Mat. Res. Symp. Proc.* **140** (1989) 309.
23. S. M. HSU, Y. S. WANG and R. G. MUNRO, "*Wear of materials*", (American Society for Mechanical Engineers, New York, 1989) 723.
24. N. P. PADTURE and H. M. CHAN, *J. Amer. Ceram. Soc.* **75** (1992) 1870.
25. C. A. POWELL-DOGAN and A. H. HEUER, *ibid.* **73** (1990) 3677.
26. *Idem., ibid.* **73** (1990) 3684.
27. C. A. POWELL-DOGAN, A. H. HEUER, M. J. READEY and K. MERRIAM, *ibid.* **74** (1991) 646.
28. W. WONG-NG, S. W. FREIMAN, C. R. HUBBARD, B. J. HOCKEY, S. WEISSMANN and C. S. LO, in Proceedings of the First International Conference on Ceramic Powder Processing Science, Orlando, FL, edited by G. L. Messing, E. R. Fuller Jr. and H. Hausner (The American Ceramic Society, Westerville, Ohio 1988) p. 1183.
29. S. W. WIEDERHORN, B. J. HOCKEY and R. F. KRAUSE Jr. and K. JAKUS, *J. Mater. Sci.* **21** (1986) 810.

Received 16 September
and accepted 8 October 1993